

Supporting Information

Conformational heterogeneity in a fully-complementary DNA three-way junction with a GC-rich branchpoint

Anita Toulmin, Laura E. Baltierra-Jasso, Michael J. Morten, Tara Sabir, Peter McGlynn, Gunnar F. Schröder, Brian O. Smith and Steven W. Magennis*

*E-mail: steven.magennis@glasgow.ac.uk

SUPPLEMENTARY FIGURES

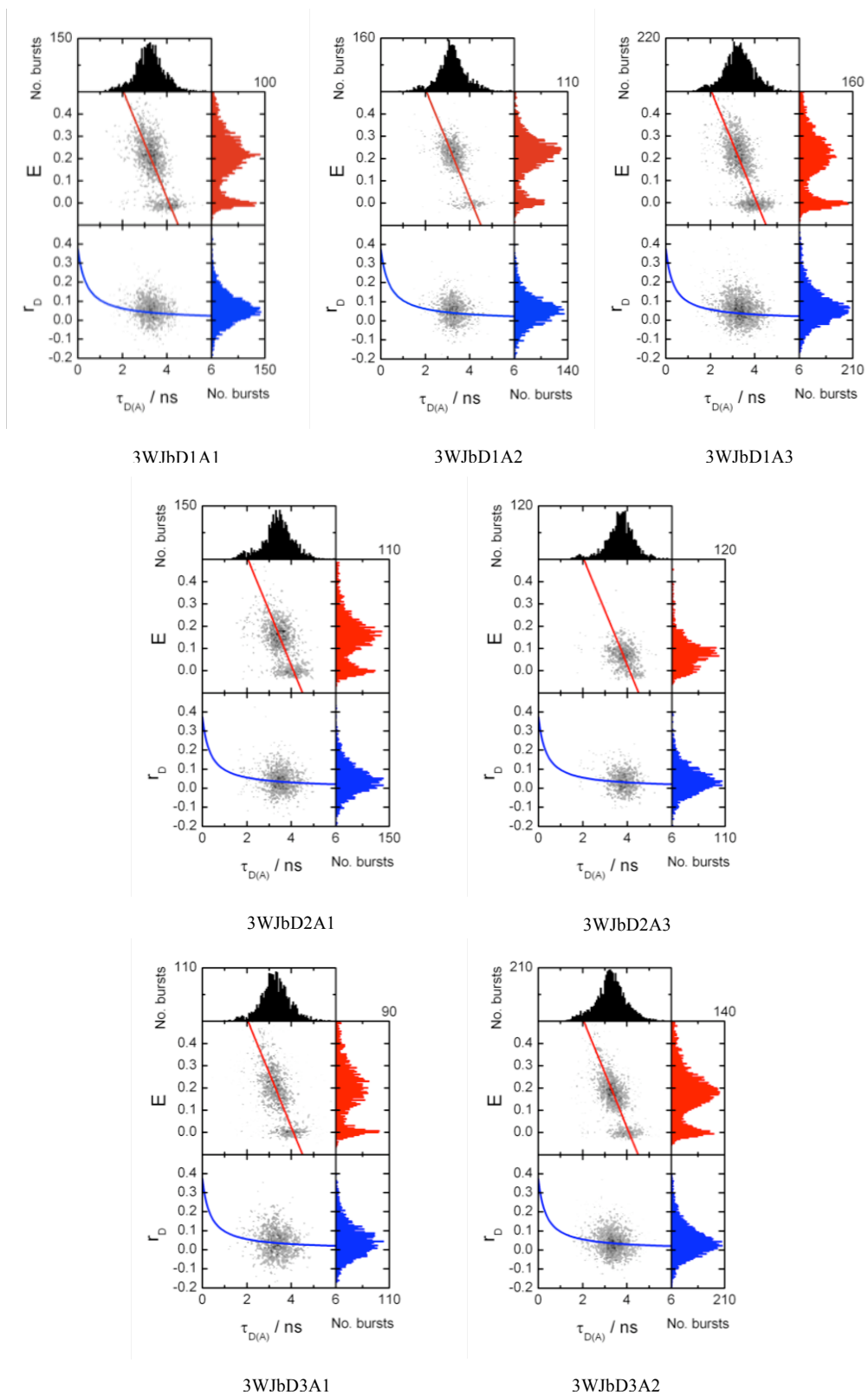


Figure S1. Single-molecule FRET plots for 3WJb in a buffer containing 0 mM MgCl₂ (see Fig. 1 for labeling positions).

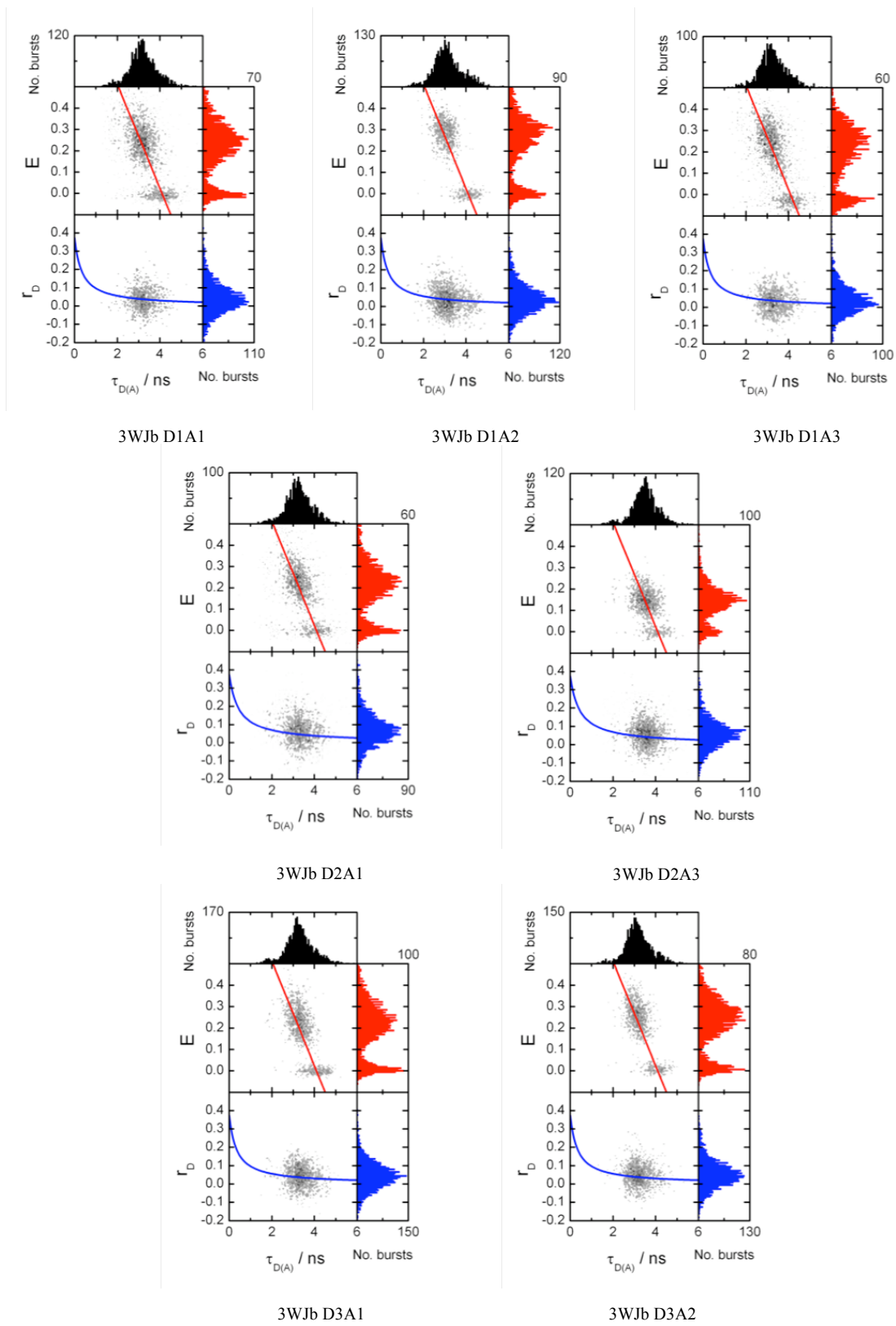
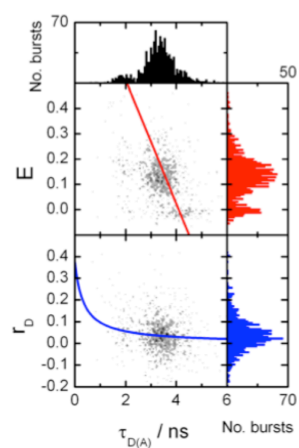
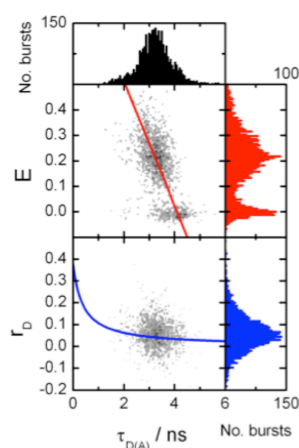


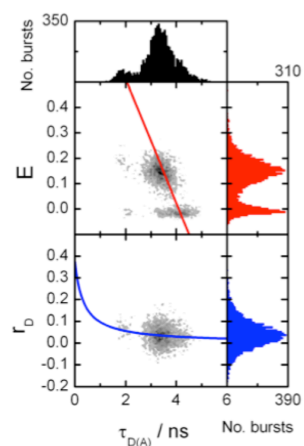
Figure S2. Single-molecule FRET plots for 3WJb in a buffer containing 1 mM MgCl₂ (see Fig. 1 for labeling positions).



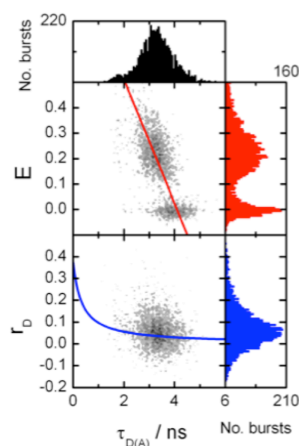
3WJa D1A1 0mM



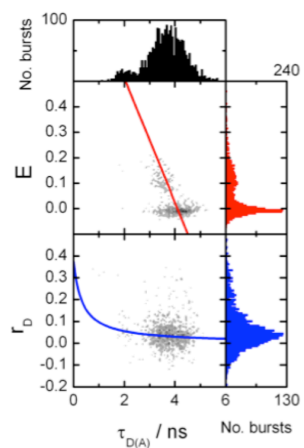
3WJb D1A1 0mM



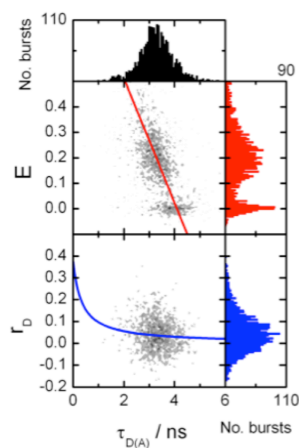
3WJa D1A3 0mM



3WJb D1A3 0mM

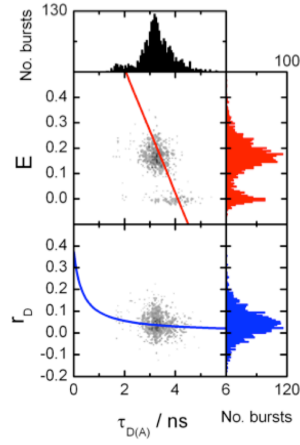


3WJa D3A1 0mM

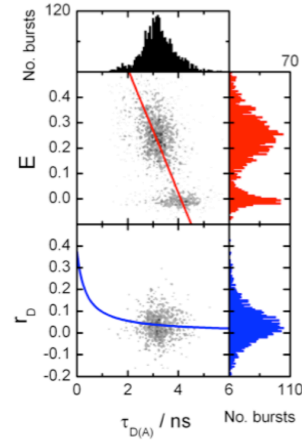


3WJb D3A1 0mM

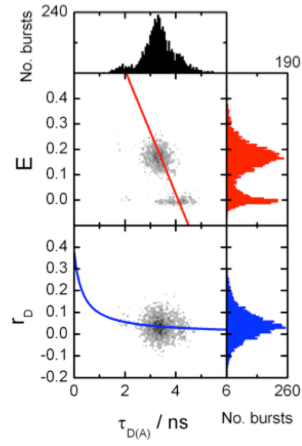
Figure S3. Comparison between single-molecule FRET plots for 3WJa (left) and 3WJb (right) for the FRET pairs D1A1 (top), D1A3 (middle) and D3A1 (bottom) in a buffer containing 0 mM MgCl₂ (see Fig. 1 for labeling positions).



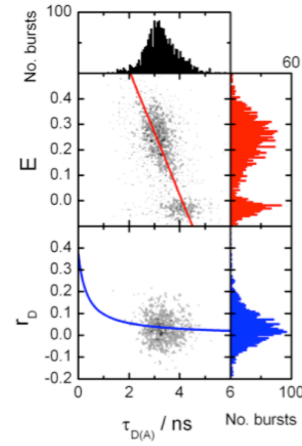
3WJa D1A1 1mM



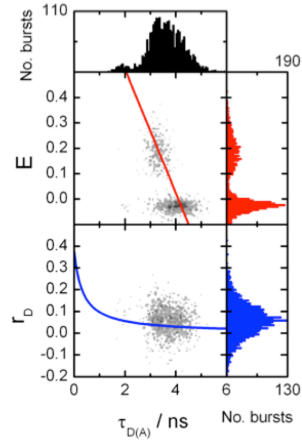
3WJb D1A1 1mM



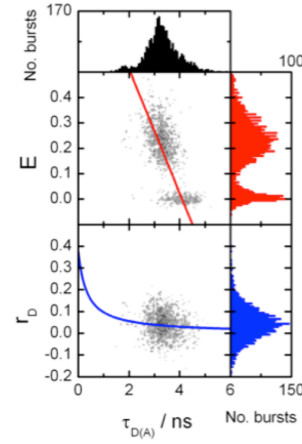
3WJa D1A3 1mM



3WJb D1A3 1mM



3WJa D3A1 1mM



3WJb D3A1 1mM

Figure S4. Comparison between single-molecule FRET plots for 3WJa (left) and 3WJb (right) for the FRET pairs D1A1 (top), D1A3 (middle) and D3A1 (bottom) in a buffer containing 1 mM MgCl_2 (see Fig. 1 for labeling positions).

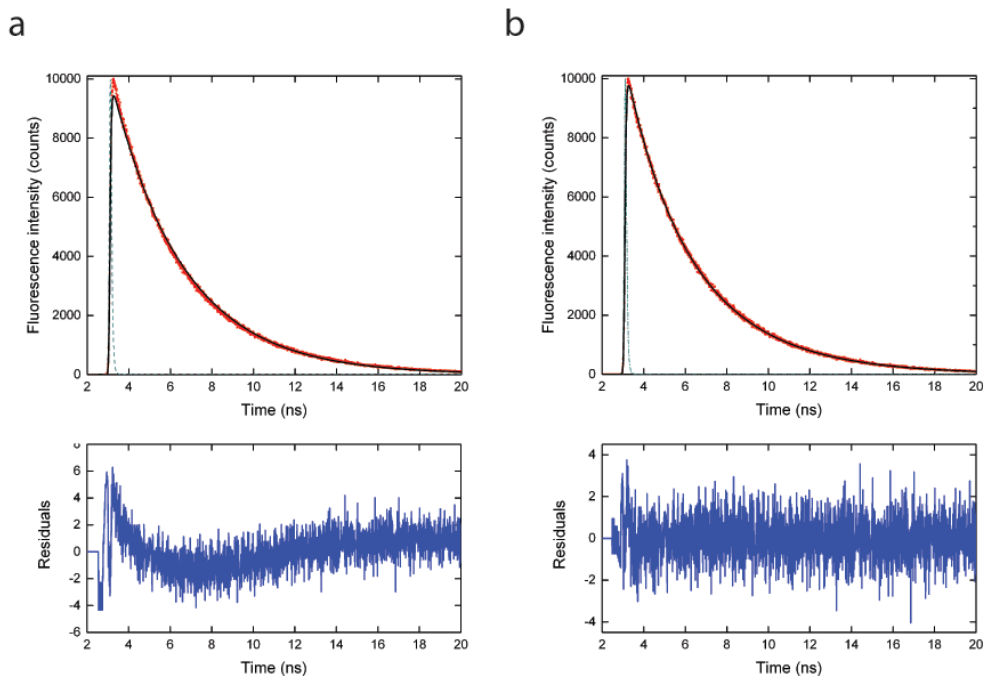


Figure S5. TCSPC for 3WJb (with dyes in the position D1 and A1) in a buffer containing 1 mM MgCl_2 , showing (a) monoexponential fit. $\tau = 3.41$ ns; $\chi^2 = 2.64$ and (b) biexponential fit. $\tau_1 = 3.78$ ns ($A_1 = 0.77$) and $\tau_2 = 1.74$ ns ($A_2 = 0.23$); $\chi^2 = 1.04$. The top panel shows the raw data in black, the instrument response function in green and the fit in red; the bottom panel shows the residuals in blue.

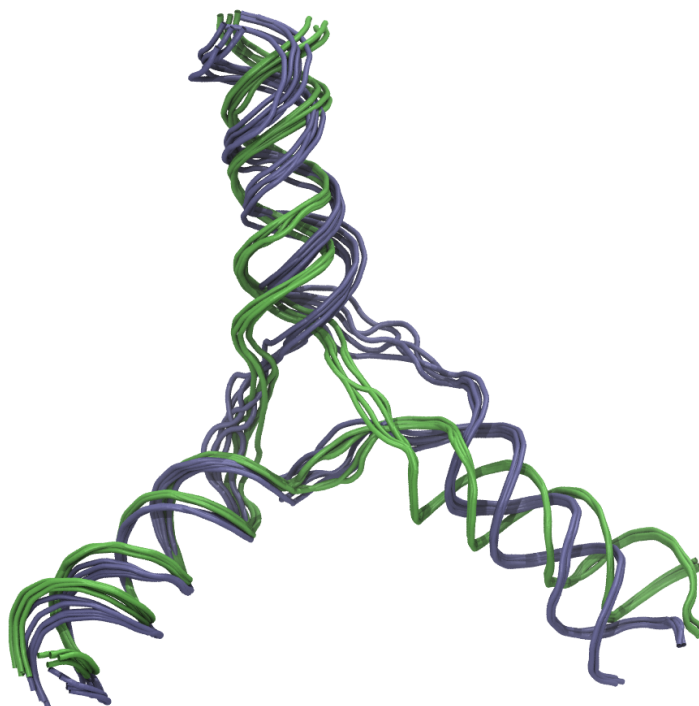


Fig. S6. Global structure of 3WJb derived from SM-FRET distance restraints for the major FRET population and MD simulations showing that the global structures for 3WJa (blue) and the major conformation of 3WJb (green) are similar in a buffer containing 0 mM MgCl_2 ; the five lowest energy conformations are overlaid.

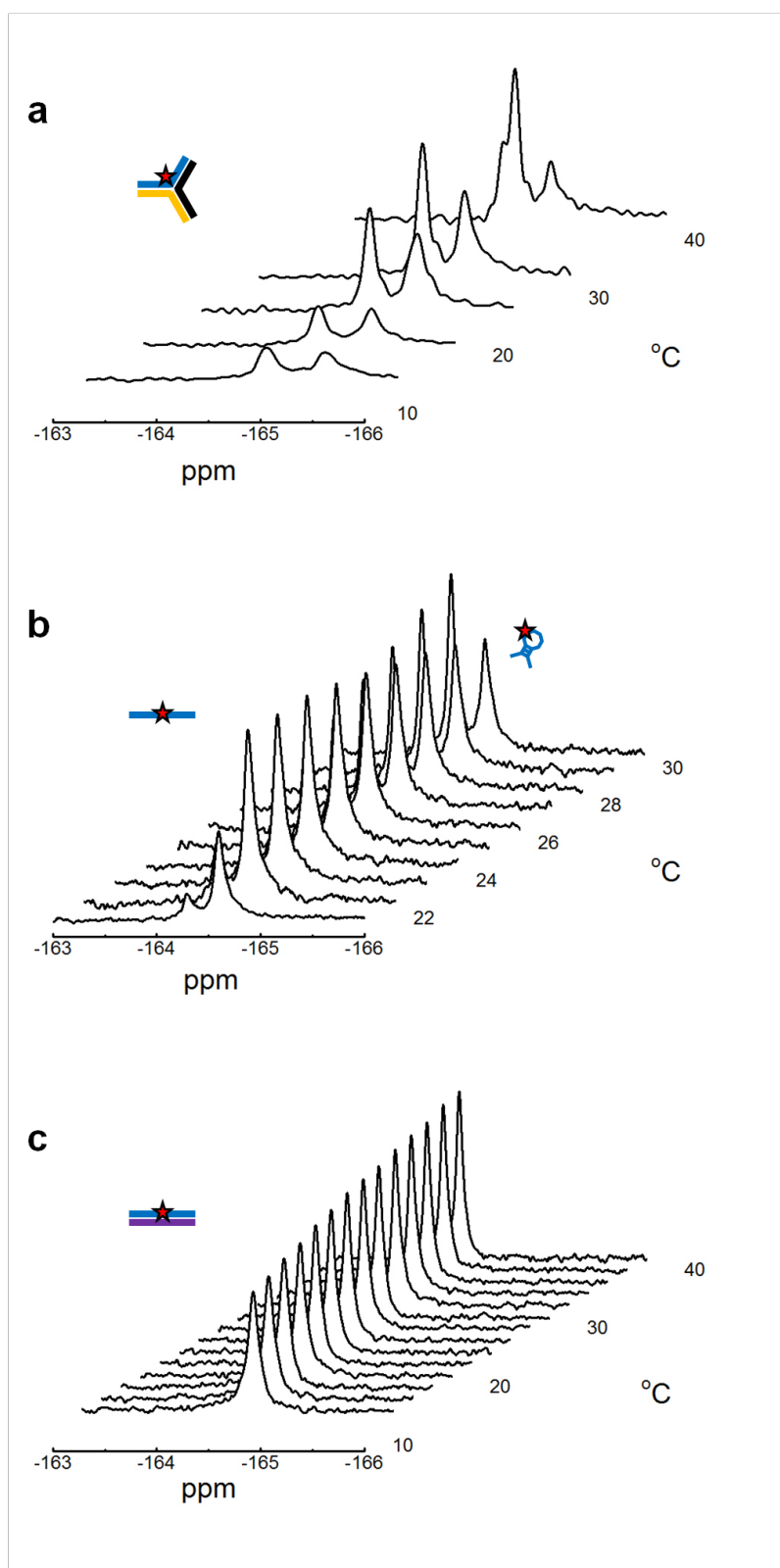


Fig. S7. The 1D ^{19}F NMR spectra of (a) a GC rich 3WJ in D_2O from 12-40 $^{\circ}\text{C}$, (b) ssDNA in H_2O from 21-30 $^{\circ}\text{C}$ and (c) dsDNA in H_2O from 12-38 $^{\circ}\text{C}$ are shown. Similarities between the 3WJ in H_2O (Fig. 4) and D_2O indicate that the fine structure of

S8

the peaks seen in H₂O are due to the structure of the 3WJ rather than arising from secondary isotope effects. The ssDNA ¹⁹F NMR spectrum in (b) shows two peaks across all temperatures that correspond to two distinct ssDNA conformations. The distributions between these populations shift to favour the more downfield peak at higher temperatures, indicating that this chemical shift originates from a ssDNA conformation that has no defined secondary structure.

Supplementary Tables

Table S1. Sub-ensemble analysis of MFD data for 3WJb in buffer containing 0 mM MgCl₂. The whole FRET population was analyzed.

FRET pair	τ_1 / ns	A₁	τ_2 / ns	A₂	Fit to peak / ns*
D1A1 (0mM)	1.93	0.23	3.24	0.77	3.20
D1A3 (0mM)	2.23	0.34	3.26	0.66	3.13
D3A1 (0mM)	1.96	0.17	3.27	0.83	3.25

* Single Gaussian fit to a smaller sub-ensemble region from MFD data in Fig. S1 centered on the FRET maximum (the selected region of 0.7 ns vs. 0.07 E).

Table S2. DRMSD to the FRET based distance restraints for the calculated 3WJb structures with different branchpoint base pairing restraints. The mean DRMSD and standard deviations for each ensemble of 5 lowest energy structures to the FRET based distance restraints are shown.

Ensemble	DRMSD(SD) in 0 mM Mg²⁺ (Å)	DRMSD(SD) in 1 mM Mg²⁺ (Å)
0-free	1.27 (0.02)	0.94 (0.02)
1-free	0.74 (0.02)	0.54 (0.04)
2-free	0.36 (0.05)	0.51 (0.01)
3-free	0.47 (0.02)	0.21 (0.03)